

Available online at [www.sciencedirect.com](http://www.sciencedirect.com)

ScienceDirect

journal homepage: [www.elsevier.com/locate/he](http://www.elsevier.com/locate/he)

# Electrodes modified with Ni electrodeposition decrease hexavalent chromium generation in an alkaline electrolysis process

Froylan Alonso Soriano Moranchell <sup>a</sup>, Juan Manuel Sandoval Pineda <sup>a</sup>,  
Jesús Nahúm Hernández Pérez <sup>b</sup>, Usiel Sandino Silva-Rivera <sup>a</sup>,  
Claudia Alicia Cortes Escobedo <sup>c</sup>, Rosa de Guadalupe González Huerta <sup>b,\*</sup>

<sup>a</sup> Instituto Politécnico Nacional-ESIME-Azc, SEPI, Av. De las Granjas, No. 682, Azcapotzalco, CP 02250, CDMX, Mexico

<sup>b</sup> Instituto Politécnico Nacional -ESIQIE, Laboratorio de Investigación de Electroquímica, UPALM, CP 07738, CDMX, Mexico

<sup>c</sup> Instituto Politécnico Nacional-CIITEC, Cda. Cecati s/n, Col. Sta. Catarina, Azcapotzalco, CP 02250, CDMX, Mexico

## HIGHLIGHTS

- One of the challenges to widespread use of water electrolysis is to reduce maintenance time.
- $\text{Cr}^{6+}$  was detected out of norm in electrolyte using stainless steel electrodes.
- $\text{Cr}^{6+}$  is very dangerous metal ion, generates different types of cancer in people.
- In modified Ni electrodes,  $\text{Cr}^{6+}$  was detected within norm in the electrolyte.
- Electrode materials must be stable at high anodic potential and alkaline media.

## ARTICLE INFO

### Article history:

Received 21 July 2019

Received in revised form

9 December 2019

Accepted 6 January 2020

Available online xxx

### Keywords:

Alkaline electrolyser

Hydrogen

Hexavalent chromium

Modified electrodes

Ni-electrodeposited electrode

## ABSTRACT

Alkaline water electrolysis is one of the easiest methods used to produce hydrogen, offering the advantages of simplicity and low cost. The challenges for the widespread use of water electrolysis are to reduce energy consumption, cost and maintenance and to increase the reliability, durability and safety of the process. The alkaline electrolysis of water has been used for many years to obtain  $\text{H}_2$  and  $\text{O}_2$ ; however, less expensive, more active, durable and efficient electrodes must be designed. Stainless steel (SS) is considered one of the least expensive electrode materials for alkaline electrolyzers, since it is relatively chemically stable and has a low overpotential. Nevertheless, SS anodes do not withstand high concentration alkaline solutions because they undergo a corrosion process. If the electrolyser operates at a voltage of up to 1.6 V, it can generate  $\text{Fe}_3\text{O}_4$  and hazardous hexavalent chromium ( $\text{Cr}^{6+}$ ) at the anode. Hexavalent chromium is generated when the chromium-containing stainless steel electrodes undergo an electro-oxidation process. In this work, a low power alkaline electrolyser was designed. In the first step, six electrodes were manufactured of stainless steel. In the second step, a nickel layer with matte or opaque finish was deposited on the SS surfaces to improve their resistance to corrosion and wear. Then, the performance curves and the production of hexavalent chromium were determined. The performance curve after 70 h of operation with nickel-plated electrodes showed an overpotential of 0.5 V at 10 A compared with stainless steel electrodes.  $\text{Cr}^{6+}$  was

\* Corresponding author.

E-mail address: [rgonzalez@ipn.mx](mailto:rgonzalez@ipn.mx) (R.G. González Huerta).

<https://doi.org/10.1016/j.ijhydene.2020.01.050>

0360-3199/© 2020 Hydrogen Energy Publications LLC. Published by Elsevier Ltd. All rights reserved.

detected in the electrolyte and bubbler water of the system using SS electrodes at values that exceeded the standard ( $>0.5\text{--}1\text{ mg L}^{-1}$ ). If the electrolyser used Ni-electrodeposited electrodes,  $\text{Cr}^{6+}$  was observed in quantities within the normal range ( $<0.1\text{ mg L}^{-1}$ ). It is very important to prepare modified anodes with nickel electro-deposited, this process prevents the generation of hexavalent chromium, contamination of the electrolyte and reduces maintenance times. The above compensates the slight increase in electrodes cost and energy consumed by the electrolyser.

© 2020 Hydrogen Energy Publications LLC. Published by Elsevier Ltd. All rights reserved.

## Introduction

Alkaline water electrolysis is an inexpensive method for hydrogen production, offering the advantage of simplicity. The challenges preventing the widespread use of water electrolysis are to reduce its energy consumption, cost and maintenance and to increase its reliability, durability and safety. Alkaline electrolysis in water has been used for many years to generate  $\text{H}_2$  and  $\text{O}_2$ . However, less expensive, more active and robust cathodic and anodic electrodes must be designed.

Water electrolysis comprises two reactions: a hydrogen evolution reaction (HER) at the cathode and an oxygen evolution reaction (OER) at the anode. Both reactions must have a low overpotential to increase the efficiency. The overvoltage of the OER has been identified as the greatest source of energy loss in water electrolysis. In addition, the anode can undergo electrocorrosion processes, resulting in higher overpotentials and shorter lifetimes [1]. This overpotential is directly related to the potential difference necessary to drive the system at a higher current density, and therefore, is directly related to the cost of the hydrogen production, as an alkaline electrolyser can operate at  $0.2\text{--}0.4\text{ A cm}^{-2}$  [2].

Stainless steel is considered one of less expensive electrode materials used for alkaline electrolyzers. Stainless steel (304 and 316) is composed of 18–22% w of Cr, 8–11% Ni and 2% Mo. Stainless steel is chemically stable in alkaline medium, but when a potential  $>1.6\text{ V}$  is applied between electrodes, corrosion processes occur at the anode. A low potential (1.6 V) must be applied to minimize this corrosion process, but the typical voltage normally ranges from 1.8 to 2.4 V for the monopolar configuration of an electrolysis system [3].

Articles analyzing the corrosion processes and determining the compounds generated during operation of a low power alkaline electrolyser were not identified in a literature search. Some electrolyser designs have been discussed in the literature. For example, Lavorante MJ et al. [4] evaluated the performance of four different kinds of stainless steel 316L mechanized electrodes, which were used in alkaline water electrolyzers for hydrogen production. El-Kassaby MM et al. [5] constructed a simple and innovative HHO generation system using stainless steel plates as the electrodes, and the optimized parameters were the number of neutral plates, the distance between the plates and the electrolyte type (NaOH or KOH). Pérez-Alonso FJ et al. [6] prepared Ni/Fe electrodes by electrodeposition on different substrates; the OER overpotential appeared to be lower for the electrodes with higher

Ni concentrations, as the  $\text{Ni}_{75}\text{Fe}_{25}\text{-Nf}$  electrode exhibited the better configuration to obtain the lowest overpotentials (2.1 V) and displayed high stability as the anode after 70 h of operation in water alkaline electrolysis. Hammoudi M et al. [7] presented a multiphysics model used for the design and diagnosis of the alkaline electrolyzers. Sandeep KC et al. [8] postulated that commercial hydrogen production by water electrolysis is limited by the high cost of electricity. In that study, porous nickel electrodes were manufactured manually on a laboratory scale. Ziemis C et al. [9] developed two pressurized alkaline electrolyser prototypes that were built to investigate the effects of different temperatures and pressures. Khalilnejad A et al. [10] designed a small alkaline electrolyser with a 25% alkaline (KOH) solution and maximum power of 60 W, and they integrated a hybrid wind-photovoltaic hydrogen system. Amores E et al. [11] designed new advanced alkaline electrolyzers that were integrated with renewable energy sources. Other studies have also described electrolyser designs [12–14] and dual combustion, hydrocarbon-hydrogen, in an internal combustion engine [15–23].

Nickel is considered the most suitable material for alkaline electrolyzers, since it is highly chemically stable, relatively inexpensive and can be used as a catalytic material for cathodic and anodic reactions. The methods used to prepare electrodes are important factors in terms of the effects on the electrode surface properties, such as roughness and stability. One of the methods used for metal deposition over metallic substrates is electrodeposition. Material selection and electrode modifications in the cell design are important in water electrolysis. Many studies have examined Ni and Ni alloy electrodes in alkaline medium [1,24–35].

In this work, an alkaline electrolyser was designed. In the first step, six electrodes were manufactured of stainless steel. Nickel with a matte or dull finish was deposited on stainless steel surfaces in the second step to improve corrosion and wear resistance. The electrolyser performance curve and production of hexavalent chromium ( $\text{Cr}^{6+}$ ) were determined after 70 h of operation.

## Materials and methods

### Preparation of modified electrodes

Stainless steel 304 gauge 20 was used as the substrate material for the electrodes (anodes and cathodes). Nickel with a matte or dull finish was deposited on the stainless steel surfaces to

improve corrosion and wear resistance. The electrodeposition method is an electrochemical technique, in which a thin layer of metallic nickel is deposited on a substrate based on Faraday's laws. The process of electrodeposition on stainless steel consists of three steps, each involving a specific solution that requires an electrochemical system, namely:

- Cleaning:** This process includes the polishing of the base metal and anodic electrolytic cleaning (AEC) of the electrodes to eliminate dust, grease and particles remaining on the surface. In AEC, the anode is the working electrode and is placed in an alkaline electrolyte solution (3% w), and the electrolysis of water occurs at  $5\text{--}7\text{ A dm}^{-2}$ . The oxygen formed in the reaction cleans the surface by removing dirt.
- Surface pretreatment (SP):** A high degree of adhesion between the deposit and the substrate is critical in all electrodeposited applications. In this case, the adhesion of nickel onto the stainless steel support becomes a very difficult task, and a surface pretreatment is necessary before nickel deposition. Good adhesion of nickel on a stainless steel surface is achieved through an electrochemical pretreatment with solution composed of  $\text{NiCl}_2$  ( $240\text{ g L}^{-1}$ ) and  $\text{HCl}$  ( $120\text{ ml L}^{-1}$ ). In SP, the cathode is the working electrode and is placed in an acid electrolyte solution, and the electrolysis of water occurs at  $2.5\text{ V}$ . The hydrogen formed in the reaction produces an electrolytic pickling on the electrode surface.
- Deposit nickel:** The present study used the Watts method for nickel electrodeposition. An electrodeposition bath was prepared by mixing  $300\text{ g L}^{-1}\text{ NiSO}_4\cdot 6\text{H}_2\text{O}$ ,  $60\text{ g L}^{-1}\text{ NiCl}_2\cdot 6\text{H}_2\text{O}$ , and  $45\text{ g L}^{-1}\text{ H}_3\text{BO}_3$  at  $55\text{--}60\text{ }^\circ\text{C}$ , pH 4.5 at  $5.4\text{ A dm}^{-2}$  and 20 min with agitation.

The components in Watts solutions affect the quality of nickel deposition. Nickel sulfate improves conductivity and metal distribution on the substratum surface and limits the cathode current density for generating sound nickel deposits. Nickel chloride improves anode corrosion, increases the conductivity and uniformity of the coating thickness distribution and helps to refine the grain size and minimize formation of nodules. Boric acid is added for buffering purposes and affects the appearance of the deposits. Deposits may be cracked and burned at low boric acid concentrations [36].

Corrosion protection in real applications mainly depends on the thickness of the nickel layer. The thickness that should be applied depends on the specific application. For example, the thickness of the nickel layer in optical and electronic applications may be  $5\text{ }\mu\text{m}$ . The thickness may be  $7\text{ }\mu\text{m}$  to protect the product purity, such as ferrous containers. Nickel coatings on automotive components, such as hydraulic rams, cylinder liners, and shock absorbers, may be  $125\text{ }\mu\text{m}$  thick to provide corrosion and wear resistance. Equation (1) was used to calculate the thickness of the nickel layer,  $s$  in micrometers ( $\mu\text{m}$ ):

$$s = \frac{m \times 10^5}{d \times A} = \frac{1.095 \times 10^5 \times I \times t \times \eta}{8.907 \times A} = \frac{0.123 \times 10^5 \times I \times t \times \eta}{A} \quad (1)$$

where  $m$  (g) is the amount of nickel deposited at the cathode (or dissolved at the anode),  $d$  ( $8.907\text{ g cm}^{-3}$ ) is the density of nickel,  $A$  ( $\text{cm}^2$ ) is the electrode area,  $1 \times 10^5$  is the conversion

factor from cm to  $\mu\text{m}$ ,  $I$  (A) is the electric current that flows through the plating tank,  $t$  (h) is the time that the current flows, and  $\eta$  is the current efficiency ratio (95%). The proportionality constant  $1.095$  in  $\text{g/Ah}$  equals  $M/nF$ , where  $M$  is the atomic weight of nickel ( $58.69\text{ g mol}^{-1}$ ),  $n$  is the number of electrons in the electrochemical reaction (2), and  $F$  is Faraday's constant, which is equal to  $26.799\text{ A-h}$  (more commonly listed as  $96,500\text{ C}$ ).

### Physical characterization

Scanning electron microscopy (SEM) was used to determine surface morphology of the nickel plating using a Sirion FEG-SEM microscope from FEI.

X-ray diffraction (XRD) patterns were recorded to analyze the surface of stainless steel and nickel-plated electrodes after 70 h of operation using a Bruker D2 Phaser. The diffraction parameters were the diffraction angle  $2\theta$  that ranged from  $20^\circ$  to  $80^\circ$ .  $\text{Cu K}\alpha$  radiation ( $\lambda = 1.5418\text{ \AA}$ ) was used in all experiments.

### Design of the electrolyser and performance curves

The electrolyser system was designed to support at a power of up to  $100\text{ W}$ . The following parameters related to the performance must be identified to evaluate the electrolysis system: (a) cell monopolar configurations, parallel connection of the electrodes, (b) electrode gap of  $2.3\text{ mm}$  and (c) operating conditions: voltage ranging from  $1.5\text{ V}$  to  $6\text{ V}$ , applied current ranging from  $0.1\text{ A}$  to  $10\text{ A}$ , temperature of  $60\text{ }^\circ\text{C}$ , electrolyte concentration (5% w NaOH solution, deionized water was used).

In the first stage, 6 stainless steel (304-19 gauge) electrodes (3 anodes and 3 cathodes, each with an area of  $74\text{ cm}^2$ ) were in contact with a 5% w alkaline solution (NaOH); this concentration was chosen to avoid the corrosive effects of NaOH and increase the simplicity of the gas purification system. In the second stage, the electrodes were modified by electrodepositing Ni onto the stainless steel substrates. Fig. 1 shows the CAD diagram of the electrolyser.

The performance curves were obtained using a test system that included a power source, phase separator or electrolyte recirculator, bubbler, dryer, mass flow meter and electrolyser, as shown in Fig. 2. A controlled current was applied from  $0.1$  to  $10\text{ A}$ . The oxyhydrogen gas production was measured with an ALICAT flowmeter. By definition, a water electrolysis system always produces hydrogen at twice the volume of oxygen (mixture of hydrogen and oxygen is called oxyhydrogen gas). The electrolyser was operated for 70 h (at  $10\text{ A}$ ), and performance curves were obtained every 10 h.

The amount of hexavalent chromium ( $\text{Cr}^{6+}$ ) dissolved in the electrolyte and water bubbler was determined with a photometric technique using 1,5-diphenylcarbazide. The spectrophotometer (UV/VIS) is an instrument that measures the absorption of light.  $\text{Cr}^{6+}$  oxidizes 1,5-diphenylcarbazide to 1,5-diphenylcarbazone, which forms a violet-colored complex with the  $\text{Cr}^{3+}$  product. At  $550\text{ nm}$ , the extinction of the dye displays a linear relationship with the  $\text{Cr}^{6+}$  concentration. The evaluation was performed using the calibration function and a reference solution.

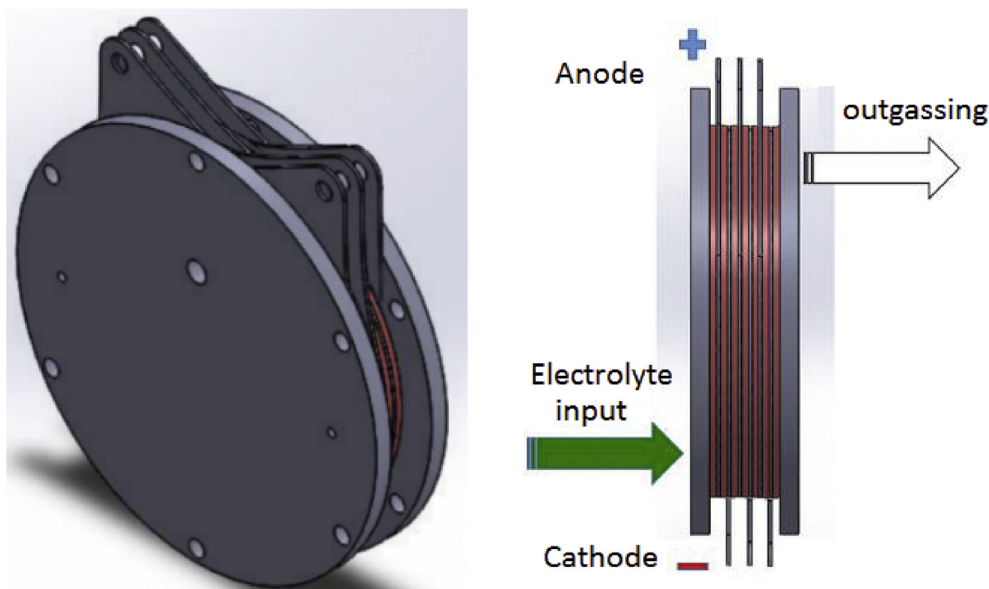


Fig. 1 – CAD diagram of the alkaline electrolyser.

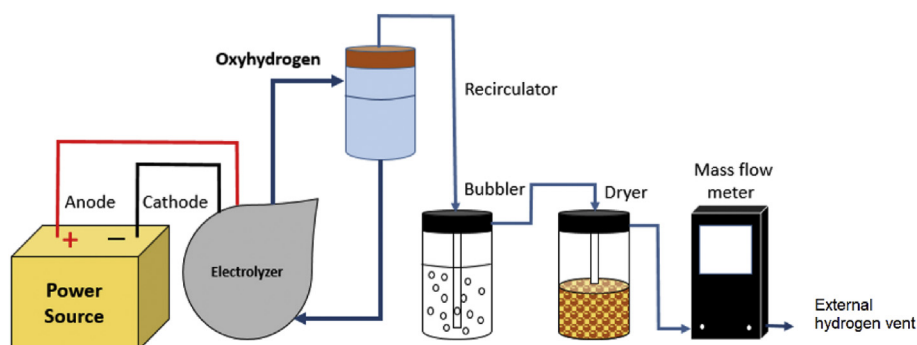


Fig. 2 – Diagram of the electrolyser test system.

## Results and discussion

### Performance electrolyser

Fig. 3 shows the stacked experimental arrangement of the electrolyser. Importantly, the electrolyser must be tested in a ventilated area without flammable materials (solvents, paper, etc.). The gas produced must be bubbled in distilled water and passed through a desiccant to remove electrolyte drag. Finally, the system must have an external hydrogen vent to avoid hydrogen accumulation in the work area.

Fig. 4(a–b) shows the performance curve of the alkaline electrolyser (EA) stack. In the initial test with stainless steel electrodes (SSE), the electrolyser required a lower voltage (4.1 V) at 10 A than nickel-electrodeposited electrodes (NiEE) (4.4 V). The performance curves were obtained every 10 h and show a decrease in the potential demand. Although no definite trend for the required voltage was observed with respect to the operating time, this lack of a trend was attributed to the superficial changes and corrosion processes of the electrodes, which will be analyzed in the next section.

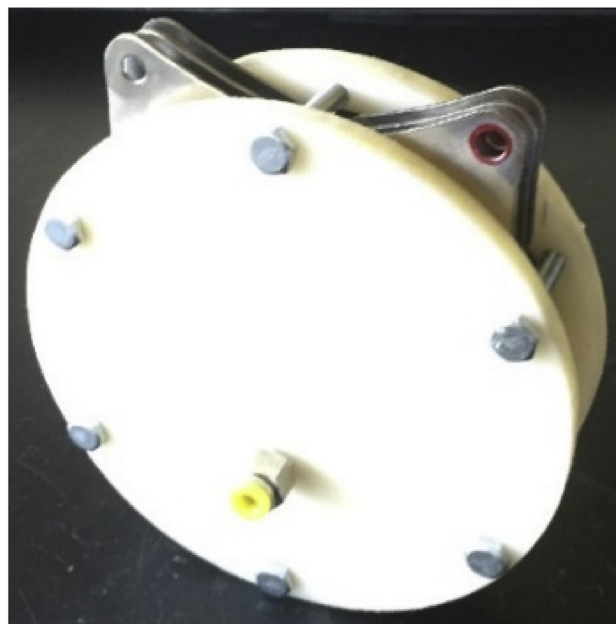


Fig. 3 – Stacked alkaline electrolyser.



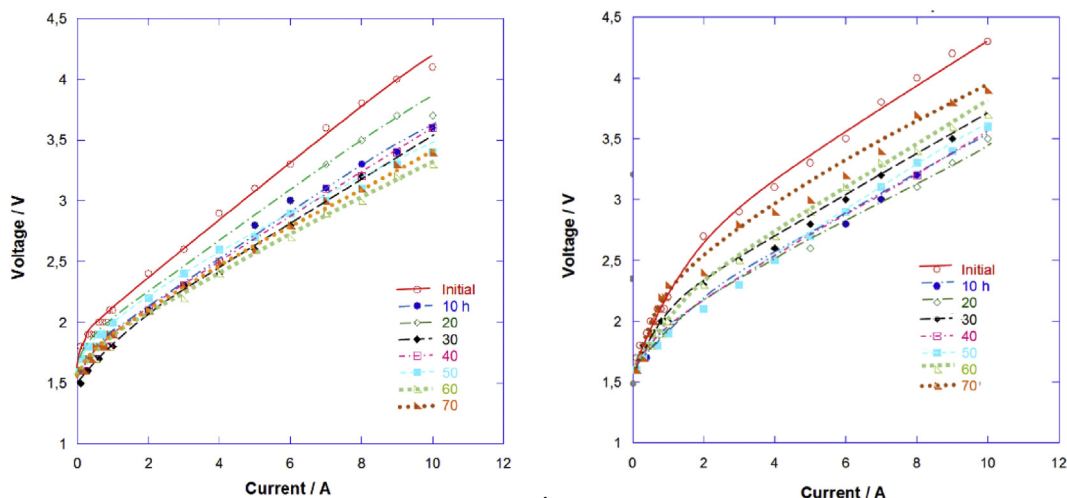
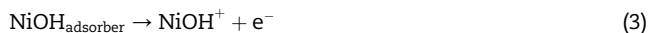


Fig. 4 – Electrolyser performance curves: a) SSE (stainless steel electrodes) and b) NiEE (nickel electrodeposited electrodes).

Fig. 5 shows the performance of electrolyser after 70 h of operation, and the voltage of the stainless steel electrodes was lower than the electrolyser with nickel-electrodeposited electrodes at 10 A. The voltage required by NiEE was higher because the nickel electrodeposited with matte finishes had a lower conductivity than that of stainless steel. According to Shreir LL. et al. [3], nickel decomposes particularly slowly in alkaline medium because it forms a passive layer. The mechanism of film formation is complex, involving the adsorption of  $\text{OH}^-$  ions to form a prepassive layer followed by dissolution, and may proceed in three consecutive steps as follows [37]:



The following reactions are responsible for the transition from active to passive behavior:



The formation of a passive layer and Ni dissolution result from the competition among these reactions. The rate-determining step changes (from 4 to 3 to 2) as the over-voltage is increased. At potentials where reactions 4 and 5 are possible, the percentage of the surface area covered with an oxide film increases, and accordingly, the current density gradually decreases in the transition region.

### Electrode analysis

An image of the stainless steel anode captured after 70 h of operation is shown in Fig. 6(a). A brown layer is observed on surface of the electrode, which was analyzed using the XRD technique. The diffractogram is shown in Fig. 6(b), and the

brown layer is iron oxide ( $\text{Fe}_2\text{O}_3$ ); therefore, if stainless steel is used as an anode in alkaline media, metallic iron is oxidized.

Fig. 7(a) shows an image of the stainless steel cathode after 70 h of operation. The electrode surface is covered by a dark layer, which was analyzed using the XRD technique. The diffractogram is shown in Fig. 7(b), and the dark layer is tetra-tenite (intermetallic alloy of  $\text{Fe}_{0.5}\text{O}_7\text{Ni}_{0.49}$ ); therefore, if stainless steel is used as an anode in alkaline media, iron and nickel are leached or dissolved (with different oxidation states:  $\text{Ni}^{2+}$ ,  $\text{Fe}^{2+}$ ,  $\text{Fe}^{3+}$ , etc.) and some ions are deposited on the cathode.

Fig. 8(a) shows an image of the nickel-electrodeposited electrode, and Fig. 8(b–c) show SEM images, both of which were captured before the operation of the electrolyser. Electrodeposition was homogeneous with a granular morphology,

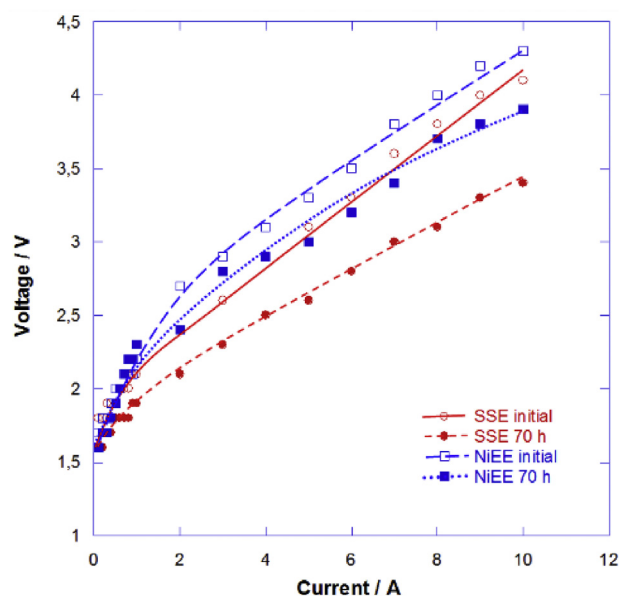


Fig. 5 – Electrolyser performance: initial results and results obtained after 70 h of operation with SSE and NiEE.

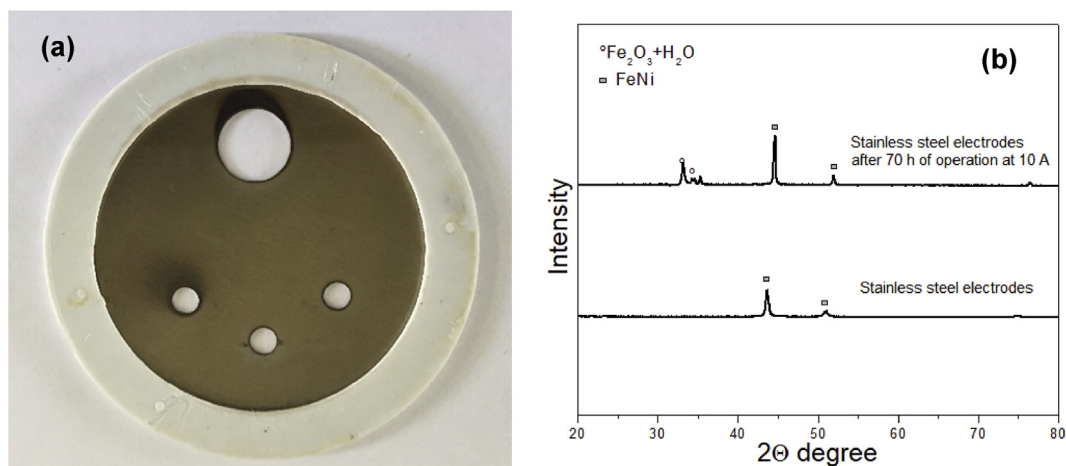


Fig. 6 – Stainless steel electrode after 70 h of operation: a) image of the anode and b) diffractogram.

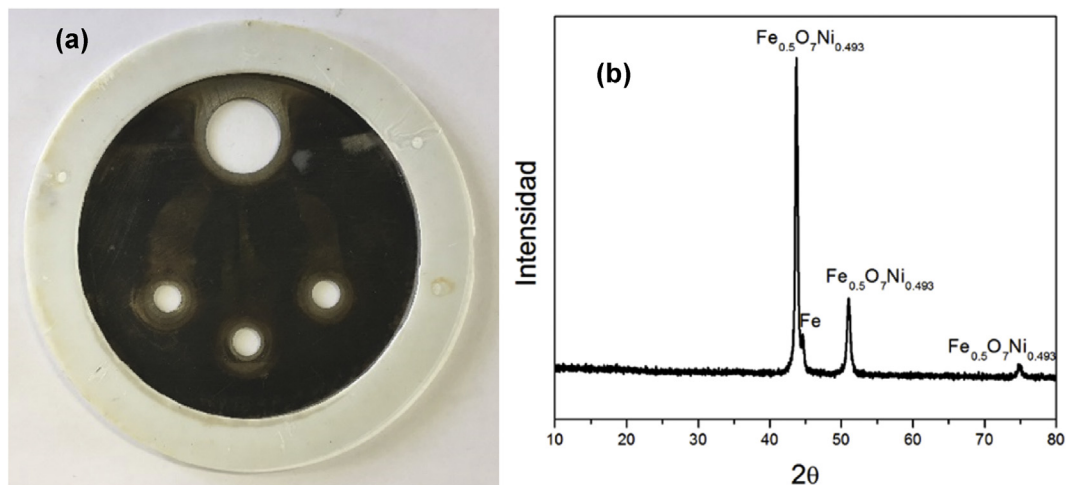


Fig. 7 – Stainless steel electrode after 70 h of operation: a) image of the cathode and b) tetraenaite diffractogram.

and the composition is shown in Fig. 8(d), which indicated 100% nickel metal.

Fig. 9 shows images of the nickel-plated electrodes (cathode and anode) after 70 h of operation. The electrode surface of the anode shows a grayish layer in Fig. 9(a), which was analyzed using the XRD technique. The diffractogram shows  $\text{Ni}(\text{OH})_2$  in Fig. 9(b), which is consistent with the findings reported by Bari et al. [37] and is described in equations (2)–(5). However,  $\text{Fe}_2\text{O}_3$  is observed less frequently than SSE. The electrode surface of cathode shows a gray layer in Fig. 9(d), which was analyzed using the XRD technique. The diffractogram shows Ni and NiO in Fig. 9(e), consistent with the results reported in the literature. The SEM images in Fig. 9(c) and (f) show a homogeneous surface, without the original granular morphology. This analysis indicates a change in the surface morphology and composition of both electrodes.

#### Electrolyte analysis

When SSEs were used, iron leached or dissolved from the anode to form a brown precipitate in the electrolyte, as shown

Fig. 10(a).  $\text{Fe}_2\text{O}_3$  was produced according to the XRD data shown in Fig. 6(b). The electrolyte showed a yellowish color, which was attributed to the generation of hexavalent chromium ( $\text{Cr}^{6+}$ ) when the chromium-containing stainless steel electrodes undergo an electro-oxidation process. When NiEEs were used, the electrolyte was clear and contained white precipitates ( $\text{NiO}$ , according to Refs. [3,37]), as shown in Fig. 10(b). Therefore, the electrolyte was analyzed with UV–vis spectroscopy to determine the amount of chromium dissolved in the electrolyte and bubbler water. Hexavalent chromium ( $\text{Cr}^{6+}$ ) is listed as compound number 16 in the Agency for Toxic Substances and Disease Registry, Priority List of Hazardous Substances (ATSDR, 1999) [38].

The solutions were analyzed after 70 h of operation. First, two 100 mL samples of bubbler water and electrolyte from the recirculator vessel were collected from both systems using SSEs and NiEEs. The Mexican regulation (NOM-002-SEMARNAT-1996) indicates that  $1 \text{ mg L}^{-1}$  of  $\text{Cr}^{6+}$  is the instantaneous maximum limit, and  $0.5 \text{ mg L}^{-1}$  is the maximum weekly average limit [39]. Table 1 shows the  $\text{Cr}^{6+}$  concentrations in the samples.

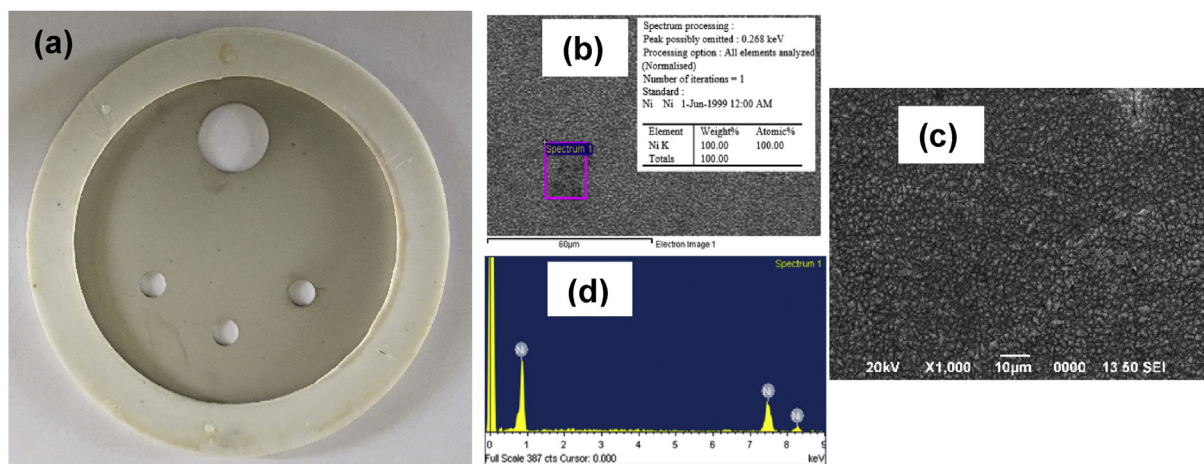


**Fig. 8 – Nickel electrodeposited electrode before the operation of the electrolyser: a) image of the cathode or anode, b) SEM image at 60 μm, c) SEM image at 10 μm, d) spectrum showing the composition of the electrodeposited Ni.**

As shown in Table 1, SSE formed  $\text{Cr}^{6+}$  at levels that exceeded the regulation in the recirculator vessel and bubbler water. This metal ion is very dangerous, and a chemical treatment is necessary to eliminate  $\text{Cr}^{6+}$ . In addition, if the electrolyser used NiEEs,  $\text{Cr}^{6+}$  was detected in quantities between the normal levels in both samples from the recirculator vessel and bubbler water. Thus, the nickel-electrodeposited

electrode generates much less  $\text{Cr}^{6+}$ . The generation of ions ( $\text{Cr}^{6+}$  and  $\text{Fe}_2\text{O}_3$ ) is attributed to defects in nickel electrodeposition, which will be reviewed and reported in future studies.

Electrode materials should be stable and should not corrode in the operating alkaline media (pH 10–14) at the required voltages (1.5–5 V) and at intermediate temperatures

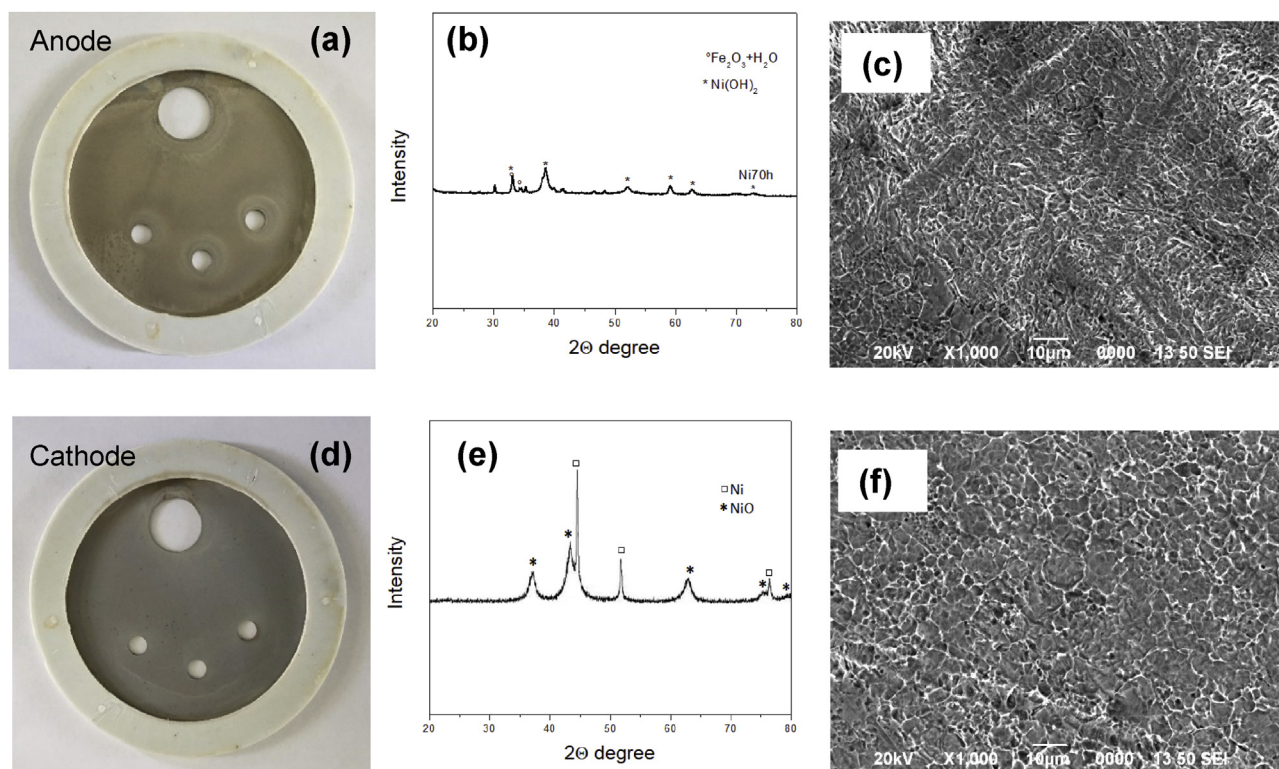


**Fig. 9 – Ni electrodeposited electrodes after 70 h of operation a) Image of the anode, b) anode diffractogram, c) SEM image of the anode, d) image of the cathode, e) cathode diffractogram, and f) SEM image of the cathode.**



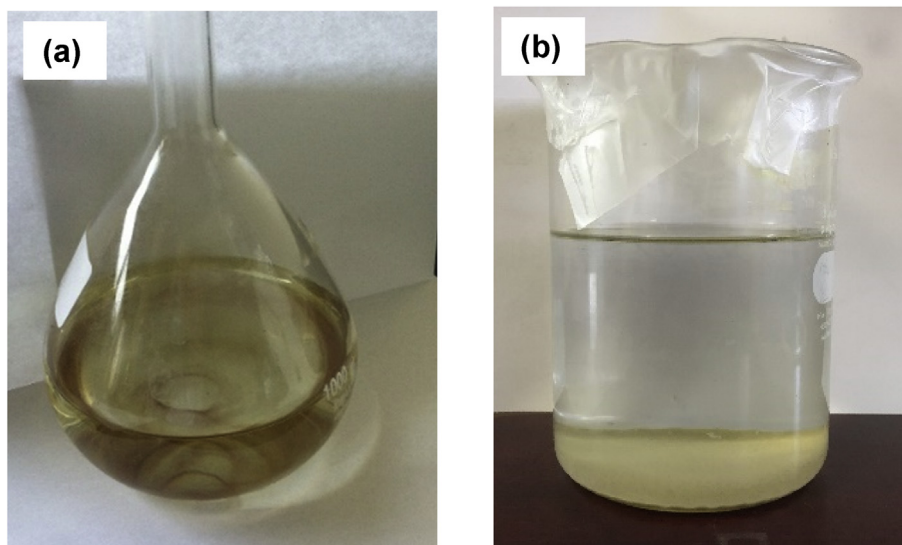
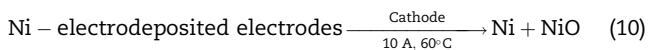
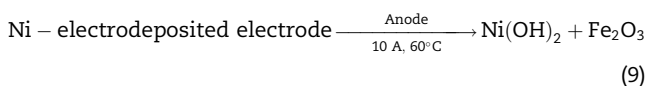
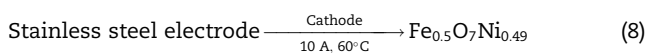
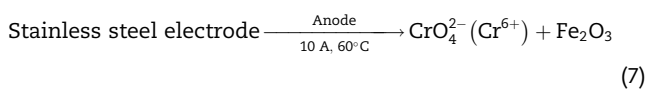


Fig. 10 – a) Electrolyte with SSE and, b) electrolyte with NiEE.

Table 1 –  $\text{Cr}^{6+}$  concentrations in the samples.

Electrolyser	Sample source	Sample	$\text{Cr}^{6+}(\text{mg L}^{-1})$
1(SSE)	Recirculator	1	1.766
1 (SSE)	Bubbler	2	0.800
2 (NiEE)	Recirculator	3	0.077
2 (NiEE)	Bubbler	4	0.019

(30–60 °C). The following compounds formed when the various electrodes were used:



It is very important to prepare modified anodes with nickel electro-deposited, this process prevents the generation of hexavalent chromium, contamination of the electrolyte and reduces maintenance times. The above compensates the increase in electrodes cost and energy consumed by the electrolyser.

## Conclusions

The challenges that must be overcome prior to the widespread use of water electrolysis are to reduce the energy consumption, cost and maintenance and to increase the reliability, durability and safety of the process. The performance curve generated after 70 h of operation with nickel-plated electrodes

showed an overpotential of 0.5 V at 10 A. Compared with stainless steel electrodes, the required voltage is higher for NiEEs because the nickel electrodeposited with matte finishes had a lower conductivity than the stainless steel. The SEM and XRD analyses indicate a change in the surface morphology and composition of both electrodes after the electrolysis process. With stainless steel electrodes (SSE) Hexavalent chromium was detected in the electrolyte and bubbler water of the system using stainless steel electrodes (SSE) that exceeded the standard ( $>0.5\text{--}1 \text{ mg L}^{-1}$ ). When nickel-plated electrodes (NiEE) were used, the  $\text{Cr}^{6+}$  concentration was observed in quantities near the normative value. It is very important to prepare modified anodes with nickel electro-deposited, this process prevents the generation of hexavalent chromium, contamination of the electrolyte and reduces maintenance times. The above compensates the slight increase in electrodes cost and energy consumed by the electrolyser.

This study is expected to serve as a reference for the proper design of low power alkaline electrolyzers, and stable and nonhazardous materials should always be used to construct the electrodes.

## Acknowledgements

The authors acknowledge the financial support from IPN multidisciplinary project SIP-2024 (2019–2020) and CONACYT: CEMIE-Ocean project 249795: Transversal Line I-LT1 and Basic Science Project A1-S-15770. The authors acknowledge Dra. Mabel Vaca Mier from UAM-Azc for the support of the hexavalent chromium determination.

## REFERENCES

- [1] Kjartansdóttir CK, Nielsen LP, Møller P. Development of durable and efficient electrodes for large-scale alkaline water



- electrolysis. *Int J Hydrogen Energy* 2013;38:8221–31. <https://doi.org/10.1016/j.ijhydene.2013.04.101>.
- [2] Ge X, Sumboja A, Wu D, An T, Li B, Goh F, Hor T, Zong Y, Liu Z. *ACS Catal* 2015;5:4643–67. <https://doi.org/10.1021/acscatal.5b00524>.
  - [3] Shreir LL, Jarman RA, Burstein GT. In: *Metal/environment reaction, corrosion*. 3rd ed., vol 1. London, UK: Newnes–Butterworths; 2000. reprinted 2000.
  - [4] Lavorante MJ, Franco JI. Performance of stainless steel 316L electrodes with modified surface to be use in alkaline water electrolyzers. *Int J Hydrogen Energy* 2016;41:9731–7. <https://doi.org/10.1016/j.ijhydene.2016.02.096>.
  - [5] EL-Kassaby MM, Eldrainy YA, Khidr ME, Khidr KI. Effect of hydroxy (HHO) gas addition on gasoline engine performance and emissions. *Alexandria Eng J* 2016;55:243–51. <https://doi.org/10.1016/j.aej.2015.10.016>.
  - [6] Pérez-Alonso FJ, Adán C, Rojas S, Peña MA, Fierro JLG. Ni/Fe electrodes prepared by electrodeposition method over different substrates for oxygen evolution reaction in alkaline medium. *Int J Hydrogen Energy* 2014;39:5204–12. <https://doi.org/10.1016/j.ijhydene.2013.12.186>.
  - [7] Hammoudi M, Henao C, Agbossou K, Dubé Y, Doumbia ML. New multi-physics approach for modelling and design of alkaline electrolyzers. *Int J Hydrogen Energy* 2012;37:13895–913. <https://doi.org/10.1016/j.ijhydene.2012.07.015>.
  - [8] Sandeep KC, Kamath S, Mistry K, Kumar AM, Bhattacharya SK, Bhanja K, Mohan S. Experimental studies and modeling of advanced alkaline water electrolyser with porous nickel electrodes for hydrogen production. *Int J Hydrogen Energy* 2017;42:12094–103. <https://doi.org/10.1016/j.ijhydene.2017.03.154>.
  - [9] Ziems Ch, Tannert D, Joachim H, Krautz A. Project presentation: design and installation of advanced high pressure alkaline electrolyzer-prototypes. *Energy Procedia* 2012;29:744–53. <https://doi.org/10.1016/j.egypro.2012.09.087>.
  - [10] Khalilnejad A, Riahy GH. A hybrid wind-PV system performance investigation for the purpose of maximum hydrogen production and storage using advanced alkaline electrolyzer. *Energy Convers Manag* 2014;80:398–406. <https://doi.org/10.1016/j.enconman.2014.01.040>.
  - [11] Amores E, Rodriguez J, Carreras Ch. Influence of operation parameters in the modeling of alkaline water electrolyzers for hydrogen production. *Int J Hydrogen Energy* 2014;39:13063–78. <https://doi.org/10.1016/j.ijhydene.2014.07.001>.
  - [12] Marini S, Salvi P, Nelli P, Pesenti R, Villa A, Berrettoni M, Zangari G, Kiros Y. Advanced alkaline water electrolysis. *Electrochim Acta* 2012;82:384–91. <https://doi.org/10.1016/j.electacta.2012.05.011>.
  - [13] Manabe A, Kashiwase M, Hashimoto T, Hayashida T, Kato A, Hirao K, Shimomura I, Nagashima I. Basic study of alkaline water electrolysis. *Electrochim Acta* 2013;100:249–56. <https://doi.org/10.1016/j.electacta.2012.12.105>.
  - [14] Yde L, Kjartansdóttir C, Allebrod A, Mogensen F, Møller MB, Hilbert P, Dierking A. 2nd generation alkaline electrolysis: final report. *Arhus University Business and Social Science – Centre for Energy Technologies*; 2013.
  - [15] Horcasitas-Verdiguél M, Sandoval-Pineda JM, Grunstein-Ramírez BA, Terán-Balaguer LF, González-Huerta RG. Design and manufacture of ICE test module to reduce gasoline consumption using oxyhydrogen gas from an alkaline electrolyzer. *ACS Energy Fuel* 2016;30:6640–5. <https://doi.org/10.1021/acs.energyfuels.6b00709>.
  - [16] Becerra-Ruiz JD, Gonzalez-Huerta RG, Gracida A, Amaro-Reyes A, Macias-Bobadilla G. Using green-hydrogen and bioethanol fuels in internal combustion engines to reduce emissions. *Int J Hydrogen Energy* 2019;44:12324–32. <https://doi.org/10.1016/j.ijhydene.2019.02.211>.
  - [17] Trujillo-Olivares I, Soriano-Moranchel F, Álvarez-Zapata LA, González-Huerta RG, Sandoval-Pineda JM. Design of alkaline electrolyser for integration in diesel engines to reduce pollutants emission. *Int J Hydrogen Energy* 2019;44:25277–86. <https://doi.org/10.1016/j.ijhydene.2019.07.256>.
  - [18] Ouchikh S, Lounici MS, Tarabet L, Loubar K, Tazerout M. Effect of natural gas enrichment with hydrogen on combustion characteristics of a dual fuel diesel engine. *Int J Hydrogen Energy* 2019;44:13974–87. <https://doi.org/10.1016/j.ijhydene.2019.03.179>.
  - [19] Alper YA. Effects of ignition advance on a dual sequential ignition engine at lean mixture for hydrogen enriched butane usage. *Int J Hydrogen Energy* 2019;44:15575–86. <https://doi.org/10.1016/j.ijhydene.2019.04.088>.
  - [20] Tüchler S, Dimitriou P. On the capabilities and limitations of predictive, multi-zone combustion models for hydrogen-diesel dual fuel operation. *Int J Hydrogen Energy* 2019;44:18517–31. <https://doi.org/10.1016/j.ijhydene.2019.05.172>.
  - [21] Jabbar AI, Koylu UO. Influence of operating parameters on performance and emissions for a compression-ignition engine fueled by hydrogen/diesel mixtures. *Int J Hydrogen Energy* 2019;44:13964–73. <https://doi.org/10.1016/j.ijhydene.2019.03.201>.
  - [22] Dimitriou P, Tsujimura T, Suzuki Y. Low-load hydrogen-diesel dual-fuel engine operation – a combustion efficiency improvement approach. *Int J Hydrogen Energy* 2019;44:17048–60. <https://doi.org/10.1016/j.ijhydene.2019.04.203>.
  - [23] Kotten H. Hydrogen effects on the diesel engine performance and emissions. *Int J Hydrogen Energy* 2018;43:10511–9. <https://doi.org/10.1016/j.ijhydene.2018.04.146>.
  - [24] Müller ChI, Rauscher T, Schmidt A, Schubert T, Weigardner T, Kieback B, Ronntzsch L. Electrochemical investigations on amorphous Fe-base alloys for alkaline water electrolysis. *Int J Hydrogen Energy* 2014;39:8926–37. <https://doi.org/10.1016/j.ijhydene.2014.03.151>.
  - [25] Jong-Hoon K, Jung-Nam L, Chung-Yul Y, Kyo-Beum L, Woong-Moo L. Low-cost and energy-efficient asymmetric nickel electrode for alkaline water electrolysis. *Int J Hydrogen Energy* 2015;40:10720–5. <https://doi.org/10.1016/j.ijhydene.2015.07.025>.
  - [26] Schalenbach M, Kasian O, Mayrhofer KJJ. An alkaline water electrolyzer with nickel electrodes enables efficient high current density operation. *Int J Hydrogen Energy* 2018;43:11932–8. <https://doi.org/10.1016/j.ijhydene.2018.04.219>.
  - [27] Chanda D, Hnat T, Paidar M, Bouzek K. Evolution of physicochemical and electrocatalytic properties of NiCo<sub>2</sub>O<sub>4</sub> (AB<sub>2</sub>O<sub>4</sub>) spinel oxide with the effect of Fe substitution at the A site leading to efficient anodic O<sub>2</sub> evolution in an alkaline environment. *Int J Hydrogen Energy* 2014;39:5713–22. <https://doi.org/10.1016/j.ijhydene.2014.01.141>.
  - [28] Kuleshov VN, Kuleshov NV, Grigoriev SA, Udriş EY, Millet P, Grigoriev AS. Development and characterization of new nickel coatings for application in alkaline water electrolysis. *Int J Hydrogen Energy* 2016;41:36–45. <https://doi.org/10.1016/j.ijhydene.2015.10.141>.
  - [29] Rauscher T, Müller ChI, Schmidt A, Kieback B, Reontzsch L. Ni-Mo-B alloys as cathode material for alkaline water electrolysis. *Int J Hydrogen Energy* 2016;41:2165–76. <https://doi.org/10.1016/j.ijhydene.2015.12.132>.
  - [30] Gonzalez-Buch C, Herraiz-Cardona I, Ortega EM, Mestre S, Perez-Herranz V. Synthesis and characterization of Au-

- modified macroporous Ni electrocatalysts for alkaline water electrolysis. *Int J Hydrogen Energy* 2016;41:764–72. <https://doi.org/10.1016/j.ijhydene.2015.10.142>.
- [31] Solmaz R, Doner A, Dogrubas M, Erdogan IY, Kardas G. Enhancement of electrochemical activity of Raney-type NiZn coatings by modifying with PtRu binary deposits: application for alkaline water electrolysis. *Int J Hydrogen Energy* 2016;41:1432–40. <https://doi.org/10.1016/j.ijhydene.2015.11.027>.
- [32] Solmaz R, Salcı A, Yuksel H, Dogrubas M, Kardas G. Preparation and characterization of Pd-modified Raney-type NiZn coatings and their application for alkaline water electrolysis. *Int J Hydrogen Energy* 2017;42:2464–75. <https://doi.org/10.1016/j.ijhydene.2016.07.221>.
- [33] Egelund S, Caspersen M, Nikiforov A, Møller P. Manufacturing of a LaNiO<sub>3</sub> composite electrode for oxygen evolution in commercial alkaline water electrolysis. *Int J Hydrogen Energy* 2016;41:10152–60. <https://doi.org/10.1016/j.ijhydene.2016.05.013>.
- [34] Chanda D, Basu S. Electrochemical synthesis of Li-doped NiFeCo oxides for efficient catalysis of the oxygen evolution reaction in an alkaline environment. *Int J Hydrogen Energy* 2018;43:21999–2011. <https://doi.org/10.1016/j.ijhydene.2018.10.078>.
- [35] Koj M, Gimpel T, Schade W, Turek T. Laser structured nickel-iron electrodes for oxygen evolution in alkaline water electrolysis. *Int J Hydrogen Energy* 2019;44:12671–84. <https://doi.org/10.1016/j.ijhydene.2019.01.030>.
- [36] Jacobs J, Testa SM. Overview of chromium(VI) in the environment: background and history. 2004. L1608\_C01.fm.
- [37] Di Bari GA. Capítulo 3 electrodeposition of nickel. *Modern electroplating*. EUA: John Wiley & Sons Inc; 2010.
- [38] Estados Unidos de America U.S Department Of Health And Human Services. Toxicological profile of chromium. Citado el 24 de junio del 2017 en el sitio web, <https://www.atsdr.cdc.gov/toxprofiles/tp7.pdf>; 2012.
- [39] Estados Unidos Mexicanos. Secretaria de Medio ambiente y recursos naturales. 1998. NOM-002-ECOL-1996.